Bol. Soc. Esp. Mat. Apl. n° 0 (0000), 1–33

Numerical Micromagnetics: A Review

Carlos J. García-Cervera

Mathematics Department, University of California, Santa Barbara, CA 93106, USA

cgarcia@math.ucsb.edu

Version of 20 de junio de 2007

Abstract

Numerical simulation has become an important tool in the study of both static and dynamic issues in ferromagnetic materials. We present a review of some of the recent advances in numerical Micromagnetics.

Palabras clave : *Micromagnetics, Landau-Lifshitz equation.*
Clasificación por materias AMS : *65M06; 65Z05; 35Q60.*

1. Introduction

A ferromagnetic material is one that possesses spontaneous magnetization. The magnetization in ferromagnetic materials can exhibit intricate domain structures, characterized by areas where the magnetization varies slowly, separated by sharp transition layers, where the orientation of the magnetization changes on a much shorter lengthscale [1, 2]. A first attempt to explain these domain structures was carried out by Weiss [3], who introduced the idea of a molecular field responsible for the orientation of the magnetization. The quantum mechanical origin of this molecular field was discovered by Heisenberg [4], who explained it as an exchange field that tends to align the spins.

Ferromagnetic materials are typically bistable, and one can switch between different configurations using a magnetic field. For this reason, the main application of ferromagnetic materials has been in the magnetic recording industry. With the discovery of giant magneto resistance (GMR) and interlayer exchange coupling, new applications of layered magnetic structures are being considered [5, 6, 7]. Multilayers have good permanent magnet properties, and in particular, a high coercive field and approximately rectangular hysteresis loop [8]. For that reason multilayers are an integral part of magnetic

memories (MRAMs), and have been one of the most important applications of ferromagnetic thin films in the past few years.

In Micromagnetics, the quantity of interest is the *magnetization* ($\mathbf{M}$); mathematically, it is a vector field of constant length M_s. In this article we will use physical units in the international system (S.I.). The fundamental dimensions used will be that of mass (M), length (L), time (T), and current (A). With this convention, the magnetization has units of A/m, and dimensions $[\mathbf{M}] = [M_s] = AL^{-1}$. The S.I. unit for force is the *Newton* (N), and for magnetic induction the *Tesla* (T).

The domain structures observed in ferromagnetic materials are understood as either local, or global minimizers of the Landau-Lifshitz energy [1], which is the sum of several contributions:

$$F_{LL}[\mathbf{M}] = F_a[\mathbf{M}] + F_e[\mathbf{M}] + F_s[\mathbf{M}] + F_Z[\mathbf{M}]. \tag{1}$$

For a magnetic sample occupying a domain $\Omega \subset \mathbb{R}^3$, the different contributions to the energy in (1) are:

1. **Anisotropy energy:** The electronic structure of the underlying crystalline lattice induces a preferred orientation for the spins. This is described by a term of the form

$$F_a[\mathbf{M}] = \int_\Omega \Phi\left(\frac{\mathbf{M}}{M_s}\right) d\mathbf{x},$$

where $\Phi : S^2 \to \mathbb{R}^+$ is a smooth (C^∞) function. In the case of a uniaxial material, there is a preferred axis, say OX, in which case the anisotropy energy takes the form

$$F_a[\mathbf{M}] = \frac{K_u}{M_s^2} \int_\Omega \left(M_2^2 + M_3^2\right) d\mathbf{x},$$

where K_u is a material parameter (in units of J/m^3, and dimensions $[K_u] = ML^{-1}T^{-2}$).

Although only uniaxial materials will be consider in this review, materials can present other types of crystalline anisotropy, such as cubic.

2. **Exchange Energy:** The fundamental property of ferromagnetic materials is that the spins experience the presence of an exchange field that favors alignment along a common direction. This is described by an energy term of the form

$$F_e[\mathbf{M}] = \frac{C_{ex}}{M_s^2} \int_\Omega |\nabla \mathbf{M}|^2 \, d\mathbf{x}.$$

The exchange constant C_{ex} has units of J/m, and dimensions $[C_{ex}] = MLT^{-2}$.

3. **Stray Field Energy:** A magnetized sample generates a magnetic field, which can be obtained by solving the Maxwell equations [9]. We refer to this magnetic field as *stray field*, or *self-induced field*. In the absence of electrical currents and charges, the Maxwell equations for the stray field, $\mathbf{H}_s$, and the magnetic induction, $\mathbf{B}$, reduce to

$$\begin{aligned} \operatorname{div} \mathbf{B} &= 0 \\ \nabla \times \mathbf{H}_s &= 0. \end{aligned}$$

The magnetic field, magnetic induction, and magnetization are related by

$$\mathbf{B} = \mu_0 \left(\mathbf{H}_s + \mathbf{M} \right). \tag{2}$$

In (2), μ_0 is the magnetic permeability of vacuum, which has a fixed value of $\mu_0 = 4\pi \times 10^{-7} N/A^2$, and dimensions $[\mu_0] = MLT^{-2}A^{-2}$.

From the second equation in (2) it follows that $\mathbf{H}_s = -\nabla U$ for some scalar function U, usually referred to as magnetostatic potential. The first equation in (2) may therefore be rewritten as

$$\operatorname{div} \left(-\nabla U + \mathbf{M} \right) = 0, \quad \mathbf{x} \in \mathbb{R}^3, \tag{3}$$

understood in the sense of distributions, i.e., $U \in H^1(\mathbb{R}^3)$ satisfies

$$\int_{\mathbb{R}^3} \nabla U \cdot \nabla v = \int_{\Omega} \mathbf{M} \cdot \nabla v, \quad \forall v \in H^1(\mathbb{R}^3). \tag{4}$$

The stray field (or self-induced) energy is

$$F_s = \frac{\mu_0}{2} \int_{\mathbb{R}^3} |\nabla U|^2 \, d\mathbf{x}. \tag{5}$$

From (4) with $v = U$, it follows that

$$F_s[\mathbf{M}] = \frac{\mu_0}{2} \int_{\mathbb{R}^3} |\nabla U|^2 \, d\mathbf{x} = \frac{\mu_0}{2} \int_{\Omega} \mathbf{M} \cdot \nabla U \, d\mathbf{x} = -\frac{\mu_0}{2} \int_{\Omega} \mathbf{H}_s \cdot \mathbf{M}. \tag{6}$$

Equation (4) can be rewritten as

$$\Delta U = \begin{cases} \nabla \cdot \mathbf{M} & \text{in } \Omega, \\ 0 & \text{outside } \Omega, \end{cases} \tag{7}$$

together with the jump conditions

$$[U]_{|\partial\Omega} = 0, \tag{8}$$

$$\left[\frac{\partial U}{\partial \nu} \right]_{|\partial\Omega} = -\mathbf{M} \cdot \nu. \tag{9}$$

Here $[v]_{|\partial\Omega}$ represents the jump of v at the boundary of Ω:

$$[v]_{|\partial\Omega}(x) = \lim_{\substack{y \to x \\ y \in \bar{\Omega}^c}} v(y) - \lim_{\substack{y \to x \\ y \in \Omega}} v(y),$$

and ν is the unit outward normal on $\partial\Omega$. The equation can be solved explicitly [9], and the solution is given by

$$U(\mathbf{x}) = \int_\Omega \nabla N(\mathbf{x}-\mathbf{y}) \cdot \mathbf{M}(\mathbf{y})\, d\mathbf{y}. \tag{10}$$

Here $N(\mathbf{x}) = -\frac{1}{4\pi}\frac{1}{|\mathbf{x}|}$ is the Newtonian potential.

Using Plancherel's Identity [10] the stray field energy can be written in Fourier space as

$$F_s[\mathbf{M}] = \frac{\mu_0}{2}\int_{\mathbb{R}^3} \frac{(\xi\cdot\widehat{\mathbf{M}})^2}{|\xi|^2}\, d\xi. \tag{11}$$

From equation (7)-(9) or (11), we can see that the stray field energy can be thought of as a soft penalization of both the divergence of $\mathbf{M}$ in the bulk, and the normal component of $\mathbf{M}$ on the boundary of the domain.

4. **Zeeman Energy:** In the presence of an external magnetic field $\mathbf{H}_e$, the magnetization tends to align with it. This translates into an energy term of the form

$$F_Z[\mathbf{M}] = -\mu_0 \int_\Omega \mathbf{H}_e \cdot \mathbf{M}\, d\mathbf{x}. \tag{12}$$

Nota 1 *Changes in the magnetization may produce deformations in the crystalline lattice; and vice-versa. A deformation in a ferromagnetic material can induce changes in the magnetization distribution, a phenomenon known as Magnetostriction [11, 12, 13, 14]. This ability to transform magnetic energy into kinetic energy makes ferromagnetic materials good candidates for sensors and actuators. These elastic effects, however, will not be considered here.*

In what follows, we consider the Landau-Lifshitz energy

$$F_{LL}[\mathbf{M}] = \frac{K_u}{M_s^2}\int_\Omega \left(M_2^2+M_3^2\right) + \frac{C_{ex}}{M_s^2}\int_\Omega |\nabla\mathbf{M}|^2 + \frac{\mu_0}{2}\int_{\mathbb{R}^3}|\nabla U|^2 - \mu_0\int_\Omega \mathbf{M}\cdot\mathbf{H}_e. \tag{13}$$

The energy landscape of (13) is quite rich, and by now the structure of minimizers is fairly well understood [1, 15, 16, 17, 18, 19, 20, 21, 22, 23]. Examples of minimizers of (13) are shown in figures 1 and 2.

The relaxation process of the magnetization distribution in a ferromagnetic material is described by the Landau-Lifshitz equation [1],

$$\frac{\partial\mathbf{M}}{\partial t} = -\frac{\mu_0\gamma}{1+\alpha^2}\mathbf{M}\times\mathcal{H} - \frac{\mu_0\gamma\alpha}{M_s(1+\alpha^2)}\mathbf{M}\times(\mathbf{M}\times\mathcal{H}), \tag{14}$$

where $|\mathbf{M}| = M_s$ is the saturation magnetization, and is usually set to be a constant far from the Curie temperature; γ is the gyromagnetic ratio, and the first term on the right hand side is the gyromagnetic term; α is the dimensionless damping coefficient, and the second term on the right hand side is the damping

Physical Parameters for Permalloy	
K_u	$100\ J/m^3$
C_{ex}	$1.3 \times 10^{-11}\ J/m$
M_s	$8 \times 10^5\ A/m$
γ	$1.76 \times 10^{11}\ (Ts)^{-1}$
α	0.01

Table 1: Typical values of the physical parameters in the Landau-Lifshitz equation (14) for Permalloy. Permalloy is an alloy of Nickel (80%) and Iron (20%), frequently used in magnetic storage devices.

term; $\mathcal{H}$ is the local or effective field, computed from the Landau-Lifshitz free energy functional:

$$\mathcal{H} = -\frac{\delta F_{LL}}{\delta \mathbf{M}}. \tag{15}$$

Using the expression (13) for the free energy functional, we get

$$\mathcal{H} = -\frac{2K_u}{M_s^2}\left(M_2\mathbf{e}_2 + M_3\mathbf{e}_3\right) + \frac{2C_{ex}}{M_s^2}\Delta\mathbf{M} - \mu_0\nabla U + \mu_0\mathbf{H}_e. \tag{16}$$

Here the notation $\mathbf{e_2} = (0,1,0)$, and $\mathbf{e_3} = (0,0,1)$ was used. Typical values for the physical parameters in (13) are included in Table 1.

The Landau-Lifshitz equation (14) can be written equivalently as

$$\frac{\partial \mathbf{M}}{\partial t} = -\mu_0\gamma\mathbf{M}\times\mathcal{H} + \frac{\alpha}{M_s}\mathbf{M}\times\frac{\partial \mathbf{M}}{\partial t}, \tag{17}$$

known as the Landau-Lifshitz-Gilbert equation [24]. Equations (14) and (17) must be supplemented with initial ($\mathbf{M}(\mathbf{x},0) = \mathbf{M}_0(\mathbf{x})$), and boundary conditions:

$$\frac{\partial \mathbf{M}}{\partial \nu} = 0, \quad \mathbf{x} \in \partial\Omega, \tag{18}$$

where ν denotes the outward unit normal on $\partial\Omega$.

The gyromagnetic term in the Landau-Lifshitz equation (14) is a conservative term, whereas the damping term is dissipative. In the absence of damping ($\alpha = 0$), equation (14) is related to the symplectic flow of harmonic maps [25]. This equation is also known as Schrödinger map equation because of its connection to the nonlinear Schrödinger equation found by Lakshmanan and Nakamura [26]. As a result, some of the work in that area has been connected to micromagnetics [27, 28, 29, 30, 31, 32, 33, 34].

In the high damping limit ($\alpha \to \infty$), the equation is related to the heat flow for harmonic maps [35, 36, 37]. In recent years there has been a lot of work regarding the existence and regularity of solutions to the Landau-Lifshitz equation (14) [38, 39, 40, 41, 42, 43, 44, 45, 46, 47, 48, 49, 50].

Equation (14) describes the dynamics of the magnetization at $O°$K. At nonzero temperature, the effective field is customarily added a stochastic term

[51, 52, 53]. The Langevin dynamical equations are

$$\frac{\partial \mathbf{M}}{\partial t} = -\frac{\mu_0\gamma}{1+\alpha^2}\mathbf{M}\times\left(\mathcal{H}+\sqrt{\sigma}\dot{\mathcal{W}}\right) - \frac{\mu_0\gamma\alpha}{M_s(1+\alpha^2)}\mathbf{M}\times\left(\mathbf{M}\times\left(\mathcal{H}+\sqrt{\sigma}\dot{\mathcal{W}}\right)\right), \tag{19}$$

where σ is determined by the fluctuation-dissipation theorem [54, 51, 52]:

$$\sigma = \frac{2\alpha k_B T}{\mu_0^2\gamma M_s}. \tag{20}$$

In (19), $\dot{\mathcal{W}}$ represents the effect of thermal fluctuations, and it is uncorrelated, independent, Gaussian white noise, characterized by the moments

$$\left\langle \dot{\mathcal{W}}_i(t)\right\rangle = 0, \text{ and } \left\langle \dot{\mathcal{W}}_i^j(t)\dot{\mathcal{W}}_k^l(t')\right\rangle = \delta_{ik}\delta_{jl}\delta(t-t'). \tag{21}$$

In (21), $\left\langle v\right\rangle$ represents the expected value of the random variable v; k_B is the Boltzmann constant ($k_B = 1.38054\times 10^{-23}$ Joules/degree), T is the absolute temperature, and γ is the gyromagnetic ratio. The subindices in $\dot{\mathcal{W}}$ represent different spatial locations, and the superindices represent each vector component of $\dot{\mathcal{W}}$. Equation (19) must be understood in the Stratonovich sense [55, 52]. We show in Appendix A that when the equation is interpreted in the Ito sense, the length of the magnetization is not preserved.

Understanding the long term dynamics of the Landau-Lifshitz system (14) or (19) is of practical interest in the design of effective mechanisms for magnetization reversal in computer memory cells [56]. In the simulation of the magnetization reversal process, it is important to be able to resolve the different small length scales involved, in particular, magnetic domain walls, and magnetic vortices, since these are responsible for the switching anomalies observed in experiments with submicron patterned NiFe arrays [57, 58].

In this article we present a review of the new developments in the numerical simulation of the Landau-Lifshitz equation in the presence and absence of thermal effects.

1.1. Dimensionless variables

For completeness, we present a non-dimensionalization of the Landau-Lifshitz equation, which will be used in what follows. The Landau-Lifshitz energy can be written in dimensionless variables by rescaling $\mathbf{M} = M_s\mathbf{m}$, $\mathbf{H}_s = M_s\mathbf{h}_s$, $U = M_s u$, $\mathbf{H}_e = M_s\mathbf{h}_e$, $\mathbf{x} = L\mathbf{x}'$, and $F_{LL} = (\mu_0 M_s^2)F'_{LL}$:

$$F'_{LL}[\mathbf{m}] = q\int_{\Omega'}\left(m_2^2+m_3^2\right)\,d\mathbf{x}' + \epsilon\int_{\Omega'}|\nabla\mathbf{m}|^2 + \frac{1}{2}\int_{\mathbb{R}^3}|\nabla u|^2\,d\mathbf{x}' - \int_{\Omega'}\mathbf{h}_e\cdot\mathbf{m}\,d\mathbf{x}', \tag{22}$$

where $q = 2K_u/(\mu_0 M_s^2)$ and $\epsilon = 2C_{ex}/(\mu_0 M_s^2 L^2)$ are now dimensionless.

Upon rescaling time, $t = (1+\alpha^2)(\mu_0\gamma M_s)^{-1}t'$, we can write the Landau-Lifshitz equation as

$$\frac{\partial \mathbf{m}}{\partial t'} = -\mathbf{m}\times\mathbf{h} - \alpha\mathbf{m}\times\mathbf{m}\times\mathbf{h}, \tag{23}$$

where

$$\mathbf{h} = -q\,(m_2\mathbf{e}_2 + m_3\mathbf{e}_3) + \epsilon\Delta\mathbf{m} - \nabla u + \mathbf{h}_e. \tag{24}$$

The Landau-Lifshitz-Gilbert equation can be written as

$$\frac{\partial \mathbf{m}}{\partial \tilde{t}} = -\mathbf{m}\times\mathbf{h} + \alpha\mathbf{m}\times\frac{\partial \mathbf{m}}{\partial \tilde{t}}, \tag{25}$$

where we have done a different rescaling of time: $t = (\mu_0\gamma M_s)^{-1}\tilde{t}$.

The Stochastic Landau-Lifshitz equation can be written in dimensionless variables as

$$\frac{\partial \mathbf{m}}{\partial t} = -\mathbf{m}\times(\mathbf{h} + \sqrt{\eta}\dot{\omega}) - \alpha\mathbf{m}\times\mathbf{m}\times(\mathbf{h} + \sqrt{\eta}\dot{\omega}), \tag{26}$$

where

$$\eta = \frac{2\alpha k_B T}{\mu_0 M_s^2 L^3(1+\alpha^2)}, \tag{27}$$

and $\dot{\omega}$ is uncorrelated, independent, Gaussian white noise. The parameter ϵ in (27) represents the ratio of thermal energy ($\sim k_B T$), to magnetic energy ($\sim \mu_0 M_s^2 L^3$). It follows that as the dimensions of the magnetic domain are reduced, thermal effects become more important. This has important technological implications, as it may hinder the development of highly dense nano-scale megnetic devices.

2. Time-stepping Schemes for the Landau-Lifshitz Equation

The dynamics of the magnetization distribution in a ferromagnetic thin film is an interesting and important problem from both a scientific and a technological point of view. Customarily, the main interest in these films has been their application in the magnetic recording industry. More recently, interest on using them as magnetic memory devices (MRAM) has given a greater incentive to study this subject.

2.1. Method of Lines

A traditional method for the numerical simulation of a partial differential equation is the Method of Lines. The right hand side of equation (14) is discretized in space. To fix ideas, we will only consider finite difference approximations, although spectral methods or finite elements can be used as well. Let us denote by $\mathbf{M} = \{\mathbf{m}_i\}_{i\in I}$ the discrete set of unknowns, which represent the value of the magnetization at the grid points. Let us denote the discretization of the right hand side of equation (23) by $\mathbf{F}_h(\mathbf{M}, t)$:

$$(\mathbf{F}_h(\mathbf{M}, t))_i = -\mathbf{m}_i\times\mathbf{h}_i - \alpha\mathbf{m}_i\times(\mathbf{m}_i\times\mathbf{h}_i), \tag{28}$$

where

$$\mathbf{h}_i = -q\,(m_{i,2}\mathbf{e}_2 + m_{i,3}\mathbf{e}_3) + \epsilon\Delta_h\mathbf{m}_i - \nabla u_i + \mathbf{h}_e. \tag{29}$$

In (29), we consider the standard approximation to the Laplacian using centered finite differences.

Upon spatial discretization, the resulting system of ordinary differential equations is

$$\frac{d\mathbf{M}}{dt} = F_h(\mathbf{M}, t). \tag{30}$$

The system (30) can now be integrated numerically. Explicit numerical schemes, such as fourth order Runge-Kutta, or predictor-corrector schemes, with some kind of adaptive time stepping procedure, are among the most commonly used methods for the simulation of the Landau-Lifshitz equation. The numerical integration of equation (30) using the Fourth order Runge-Kutta method proceeds as follows: Give the approximation $\mathbf{M}_n$ at time t_n, define

$$\begin{aligned}
\mathbf{K}_1 &= \mathbf{F}(\mathbf{M}_n, t_n), \\
\mathbf{K}_2 &= \mathbf{F}\left(\mathbf{M}_n + \frac{\Delta t}{2}\mathbf{K}_1, t_n + \frac{\Delta t}{2}\right), \\
\mathbf{K}_3 &= \mathbf{F}\left(\mathbf{M}_n + \frac{\Delta t}{2}\mathbf{K}_2, t_n + \frac{\Delta t}{2}\right), \\
\mathbf{K}_4 &= \mathbf{F}\left(\mathbf{M}_n + \frac{\Delta t}{2}\mathbf{K}_3, t_n + \Delta t\right).
\end{aligned}$$

The magnetization at time t_{n+1} is approximated by

$$\mathbf{M}^* = \mathbf{M}_n + \frac{\Delta t}{6}\left(\mathbf{K}_1 + 2\mathbf{K}_2 + 2\mathbf{K}_3 + \mathbf{K}_4\right), \tag{31}$$

$$\mathbf{M}_{n+1} = \frac{\mathbf{M}^*}{|\mathbf{M}^*|}. \tag{32}$$

The normalization step (32) is necessary to preserve the length of the magnetization vector at each grid point. If this step is omitted, the length constraint is satisfied only to within the temporal accuracy of the numerical method.

Although explicit schemes may achieve high order of accuracy both in space and time, the time step size is severely constrained by the stability of the numerical scheme. For physical constants characteristic of Permalloy, with a cell size $\Delta x = 0.004\,\mu m$ (256 grid points in a $1\,\mu m$ long sample), and using fourth order Runge-Kutta, a time step roughly of the order $\Delta t \approx .25$ picoseconds is needed for numerical stability. If the cell size is decreased by a factor of 10, the time step Δt must be reduced by a factor of 100.

In order to overcome the stability constraint of explicit schemes, one usually resorts to implicit schemes, such as the Backward Euler method described in [59]. However, due to the strong nonlinearities present in both the gyromagnetic and damping terms in the Landau-Lifshitz equation (14), a direct implicit discretization of the system is not efficient and is difficult to implement. To illustrate the procedure, consider only the Laplacian term in the Landau-Lifshitz

equation (14):

$$\frac{\partial \mathbf{m}}{\partial t} = -\mathbf{m} \times \Delta \mathbf{m} - \mathbf{m} \times \mathbf{m} \times \Delta \mathbf{m}. \tag{33}$$

The Backward Euler method is

$$\frac{\mathbf{m}^{n+1} - \mathbf{m}^n}{\Delta t} = -\mathbf{m}^{n+1} \times \Delta_h \mathbf{m}^{n+1} - \mathbf{m}^{n+1} \times \mathbf{m}^{n+1} \times \Delta_h \mathbf{m}^{n+1}. \tag{34}$$

In order to advance the magnetization in the Backward Euler method, the nonlinear system of equations (34) must be solved at each time step. This difficulty can be ameliorated by a semi-implicit discretization such as

$$\frac{\mathbf{m}^{n+1} - \mathbf{m}^n}{\Delta t} = -\mathbf{m}^{n} \times \Delta_h \mathbf{m}^{n+1} - \mathbf{m}^{n} \times \mathbf{m}^{n} \times \Delta_h \mathbf{m}^{n+1}. \tag{35}$$

In (35), the system of equations that has to be solved at each time-step is linear, but the coefficients change between time-steps.

Both (34) and (35) are first order discretizations in time. A second order approximation can be obtained using a Crank-Nicolson discretization. For simplicity, we consider only the case when damping is absent:

$$\frac{\mathbf{m}^{n+1} - \mathbf{m}^n}{\Delta t} = -\frac{1}{2}\left(\mathbf{m}^{n+1} \times \Delta_h \mathbf{m}^{n+1} + \mathbf{m}^{n} \times \Delta_h \mathbf{m}^{n}\right). \tag{36}$$

An alternative second order approximation of this type is [60]:

$$\frac{\mathbf{m}^{n+1} - \mathbf{m}^n}{\Delta t} = -\frac{1}{2}\left(\mathbf{m}^{n} \times \Delta_h \mathbf{m}^{n+1} + \mathbf{m}^{n+1} \times \Delta_h \mathbf{m}^{n}\right). \tag{37}$$

The time stepping (37) only requires the solution of linear systems of equations, and not nonlinear systems, as in (36).

Higher order approximations can be achieved using Backward Differentiation Formula [61].

2.2. Semi-Analytic integration

In all the numerical methods described above, the unit length constraint on the magnetization vector must be imposed by performing a projection of the intermediate values, as in (32). Given that the length of the magnetization is preserved by the Landau-Lifshitz equations, it may be desirable that the numerical method employed also preserve it. In [62], this was achieved by using semi-analytical integration of equation (30), which can be written as

$$\frac{d\mathbf{m}_i}{dt} = -\mathbf{m}_i \times \mathbf{h}_i^n - \alpha \mathbf{m}_i \times (\mathbf{m}_i \times \mathbf{h}_i^n), \tag{38}$$

$$\mathbf{m}_i(t_n) = \mathbf{m}_i^n. \tag{39}$$

In (38), the effective field, $\mathbf{h}^n$, is kept constant in the interval $[t_n, t_{n+1}]$, which allows explicit integration of equation (38) between t_n and t_{n+1}. The explicit expression for $\mathbf{m}(t_{n+1})$ follows from the two following observations:

1. Given two vectors $\mathbf{m}, \mathbf{h} \in \mathbb{R}^3$, we have the following vector identity:

$$\mathbf{m} = \frac{1}{|\mathbf{h}|^2}\left((\mathbf{m},\mathbf{h})\mathbf{h} + \mathbf{h}\times(\mathbf{m}\times\mathbf{h})\right), \tag{40}$$

   i.e., $\mathbf{m}$ is completely determined by $(\mathbf{m},\mathbf{h})$, and $\mathbf{m}\times\mathbf{h}$.

2. The scalar $(\mathbf{m},\mathbf{h})$ and the vector $\mathbf{m}\times\mathbf{h}$ satisfy simple ordinary differential equations that can be solved explicitly.

Therefore we only need to obtain an expression for $(\mathbf{m},\mathbf{h})$ and $\mathbf{m}\times\mathbf{h}$, which are:

$$(\mathbf{m}^{n+1},\mathbf{h}^n) = |\mathbf{h}|\frac{(\mathbf{m}^n,\mathbf{h}^n)\cosh(\alpha|\mathbf{h}^n|(\Delta t)) + |\mathbf{h}^n|\operatorname{senh}(\alpha|\mathbf{h}^n|(\Delta t))}{(\mathbf{m}^n,\mathbf{h}^n)\operatorname{senh}(\alpha|\mathbf{h}^n|(\Delta t)) + |\mathbf{h}^n|\cosh(\alpha|\mathbf{h}^n|(\Delta t))}, \tag{41}$$

and

$$\mathbf{m}^{n+1}\times\mathbf{h}^n = \varphi(\Delta t)\mathbf{R}^T\cdot\begin{pmatrix} 1 & 0 & 0 \\ 0 & \cos(|\mathbf{h}^n|\Delta t) & -\operatorname{sen}(|\mathbf{h}^n|\Delta t) \\ 0 & \operatorname{sen}(|\mathbf{h}^n|\Delta t) & \cos(|\mathbf{h}^n|\Delta t)\end{pmatrix}\cdot\mathbf{R}\cdot\mathbf{m}^n\times\mathbf{h}^n, \tag{42}$$

where we have defined

$$\varphi(\Delta t) = e^{-\alpha\int_{t_n}^{t_{n+1}}(\mathbf{m},\mathbf{h})(t)\,dt} = \frac{1}{\frac{(\mathbf{m}^n,\mathbf{h}^n)}{|\mathbf{h}^n|}\operatorname{senh}(\alpha|\mathbf{h}^n|\Delta t) + \cosh(\alpha|\mathbf{h}^n|\Delta t)}. \tag{43}$$

The matrix $\mathbf{R}$ in (42) is an orthonormal matrix which preserves the orientation, and such that $\mathbf{R}\cdot\mathbf{h} = |\mathbf{h}|\mathbf{e}_1$:

$$\mathbf{R} = \frac{1}{|\mathbf{h}|}\begin{pmatrix} h_1 & h_2 & h_3 \\ 0 & \frac{h_3}{\sqrt{h_2^2+h_3^2}} & -\frac{h_2}{\sqrt{h_2^2+h_3^2}} \\ -\sqrt{h_2^2+h_3^2} & \frac{h_1h_2}{\sqrt{h_2^2+h_3^2}} & \frac{h_1h_3}{\sqrt{h_2^2+h_3^2}}\end{pmatrix}, \tag{44}$$

or $\mathbf{R} = \frac{\mathbf{h}}{|\mathbf{h}|}\mathbf{I}$, if $h_2 = h_3 = 0$.

Give $\mathbf{m}^n$, $\mathbf{h}^n$ is computed from (24), and $\mathbf{m}^{n+1}$ is given by

$$\mathbf{m}^{n+1} = \frac{1}{|\mathbf{h}^n|^2}\left((\mathbf{m}^n,\mathbf{h}^n)\mathbf{h}^n + \mathbf{h}^n\times(\mathbf{m}^n\times\mathbf{h}^n)\right). \tag{45}$$

The method is first order accurate in time, and explicit. Therefore, it suffers from the same time step constraints as the Runge-Kutta method described earlier. However, the shape of the time step (45) allows for a natural form of time step control [62]. This method can also be seen as an example of more general geometric integrators to be discussed in section 2.3.

2.3. Geometric Integration

Geometric integrators are methods specially designed to preserve one or more of the geometric properties of the system under consideration [63]. An example of geometric integrators are symplectic methods [64, 65], which are designed to preserve the symplectic structure of the equation.

The use of geometric integrators for the Landau-Lifshitz equation has been explored in [66, 67]. To illustrate the method, we rewrite the Landau-Lifshitz equation as

$$\frac{d\mathbf{m}_i}{dt} = \mathbf{S}(\mathbf{p}_i) \cdot \mathbf{m}_i, \tag{46}$$

where

$$\mathbf{p}_i = \mathbf{h}_i + \alpha \mathbf{m}_i \times \mathbf{h}_i, \tag{47}$$

and

$$\mathbf{S}(\mathbf{p}) = \begin{pmatrix} 0 & -p_3 & p_2 \\ p_3 & 0 & -p_1 \\ -p_2 & p_1 & 0 \end{pmatrix}, \quad \forall \mathbf{p} \in \mathbb{R}^3. \tag{48}$$

If we fix $\mathbf{p}$ at time t_n, and solve equation (46) between t_n and t_{n+1}, we get

$$\mathbf{m}_i^{n+1} = \exp\left(\mathbf{S}(\mathbf{p}_i)\Delta t\right) \cdot \mathbf{m}_i^n, \tag{49}$$

which is exactly (45). Since $\mathbf{S}\mathbf{p}_i$ is skew-symmetric, the exponential $\exp\{\mathbf{S}\mathbf{p}_i t\}$ is an orthonormal matrix, and therefore the length of the magnetization is automatically preserved by the method.

The exponential matrix can be computed using the *Rodrigues formula* [68]:

$$\exp\{\mathbf{S}(\mathbf{p})\} = \mathbf{I} + \frac{\operatorname{sen}(\|\mathbf{p}\|)}{\|\mathbf{p}\|}\mathbf{S}(\mathbf{p}) + \frac{1-\cos(\|\mathbf{p}\|)}{\|\mathbf{p}\|^2}\mathbf{S}(\mathbf{p})^2, \tag{50}$$

which follows from the fact that $\mathbf{S}(\mathbf{p})^3 = -\|\mathbf{p}\|^2\mathbf{S}(\mathbf{p})$. In [66], geometric methods of first, second, and fourth order accuracy were constructed for the Landau-Lifshitz equation.

2.4. Gauss-Seidel Projection Method

The two main difficulties in the time-stepping of the Landau-Lifshitz equation are the stiffness of the equation, and the nonlinearity. The stiffness of the equation can be handled by using an implicit time stepping procedure, and the nonlinearity is what makes this procedure difficult or impractical. Both issues where addressed in [69], where the Gauss-Seidel Projection Method (GSPM) was developed.

Because of the nature of the equation, the gyromagnetic term and the damping term require different treatment. To illustrate the method, we again consider only the Laplacian term in the Landau-Lifshitz equation (33).

When only the damping term is present, equation (33) becomes

$$\frac{\partial \mathbf{m}}{\partial t} = -\mathbf{m} \times (\mathbf{m} \times \Delta \mathbf{m}) = \Delta \mathbf{m} + |\nabla \mathbf{m}|^2 \mathbf{m}. \tag{51}$$

This equation describes the heat flow for harmonic maps. In [70], a simple projection scheme was introduced for this equation. This scheme was shown to be unconditionally stable and more efficient than other schemes used for the simulation of equation (51).

In order to motivate the GSPM, consider equation

$$\frac{\partial \mathbf{m}}{\partial t} = -\mathbf{m} \times \Delta \mathbf{m}. \tag{52}$$

To overcome the nonlinearity of the equation, consider a simple fractional step scheme:

$$\begin{aligned} \frac{\mathbf{m}^* - \mathbf{m}^n}{\Delta t} &= \Delta_h \mathbf{m}^* \\ \mathbf{m}^{n+1} &= \mathbf{m}^n - \mathbf{m}^n \times \mathbf{m}^* \end{aligned} \tag{53}$$

or

$$\mathbf{m}^{n+1} = \mathbf{m}^n - \mathbf{m}^n \times (I - \Delta t \Delta_h)^{-1} \mathbf{m}^n. \tag{54}$$

Here I is the identity matrix, and Δ_h represents an approximation to the Laplacian.

The advantage of the scheme (54) is that the implicit step is now linear, comparable to solving heat equations implicitly, and is easy to implement. It is easy to check that the scheme (54) is consistent with (52) and is first order accurate in time. However, direct numerical implementation of (54) shows that the scheme is unstable.

The key to the GSPM is the observation that, due to the vectorial product structure of the equation, a Gauss-Seidel type of technique significantly improves the stability property of explicit schemes for the Landau-Lifshitz equation [69, 71].

Consider again the Landau-Lifshitz equation:

$$\frac{\partial \mathbf{m}}{\partial t} = -\mathbf{m} \times \mathbf{h} - \alpha\, \mathbf{m} \times \mathbf{m} \times \mathbf{h}, \tag{55}$$

where

$$\mathbf{h} = -q\,(m_2 \mathbf{e}_2 + m_3 \mathbf{e}_3) + \epsilon \Delta \mathbf{m} + \mathbf{h}_s + \mathbf{h}_e. \tag{56}$$

For the splitting procedure, define the vector field:

$$\mathbf{f} = -q\,(m_2 \mathbf{e}_2 + m_3 \mathbf{e}_3) + \mathbf{h}_s + \mathbf{h}_e \tag{57}$$

Equation

$$\frac{\partial \mathbf{m}}{\partial t} = -\mathbf{m} \times (\epsilon \Delta \mathbf{m} + \mathbf{f}) - \alpha\, \mathbf{m} \times \mathbf{m} \times (\epsilon \Delta \mathbf{m} + \mathbf{f}) \tag{58}$$

in three steps:

Step 1: Implicit Gauss-Seidel.

$$\begin{aligned} g_i^n &= (I - \epsilon \Delta t \Delta_h)^{-1} (m_i^n + \Delta t f_i^n), \\ g_i^* &= (I - \epsilon \Delta t \Delta_h)^{-1} (m_i^* + \Delta t f_i^*), \qquad i = 1, 2, 3 \end{aligned} \tag{59}$$

$$\begin{pmatrix} m_1^* \\ m_2^* \\ m_3^* \end{pmatrix} = \begin{pmatrix} m_1^n + (g_2^n m_3^n - g_3^n m_2^n) \\ m_2^n + (g_3^n m_1^* - g_1^* m_3^n) \\ m_3^n + (g_1^* m_2^* - g_2^* m_1^*) \end{pmatrix} \tag{60}$$

Step 2: Heat flow without constraints.

$$\mathbf{f}^* = -Q\,(m_2^* \mathbf{e}_2 + m_3^* \mathbf{e}_3) + \mathbf{h}_s^* + \mathbf{h}_e \tag{61}$$

$$\begin{pmatrix} m_1^{**} \\ m_2^{**} \\ m_3^{**} \end{pmatrix} = \begin{pmatrix} m_1^* + \alpha\Delta t(\epsilon\Delta_h m_1^{**} + f_1^*) \\ m_2^* + \alpha\Delta t(\epsilon\Delta_h m_2^{**} + f_2^*) \\ m_3^* + \alpha\Delta t(\epsilon\Delta_h m_3^{**} + f_3^*) \end{pmatrix} \tag{62}$$

Step 3: Projection onto S^2.

$$\begin{pmatrix} m_1^{n+1} \\ m_2^{n+1} \\ m_3^{n+1} \end{pmatrix} = \frac{1}{|m^{**}|} \begin{pmatrix} m_1^{**} \\ m_2^{**} \\ m_3^{**} \end{pmatrix} \tag{63}$$

3. Computation of the Stray Field

In broad terms, the numerical methods currently used for the simulation of the Landau-Lifshitz equation can be divided into two categories, according to how the nonlocal stray field is evaluated. In the first class of methods, or PDE methods, equation (7)-(9) is solved using an appropriate discretization. The second class of methods is based on using some kind of fast summation technique to evaluate (10).

3.1. The PDE approach

The difficulty with this approach is the lack of an effective boundary condition for U. The differential equation (7) is formulated in the entire space, which has to be truncated in simulations [72, 73]. Alternatively, a boundary integral equation can be used to represent the correct boundary condition at ∂V [74, 75]. In this approach, the magnetostatic potential is decomposed into two parts: $U = U_1 + U_2$. The first part satisfies the equation

$$\begin{aligned} \Delta U_1 &= \operatorname{div} \mathbf{M}, \quad \mathbf{x} \in \Omega \\ \frac{\partial U_1}{\partial \nu} &= 0, \quad \mathbf{x} \in \partial\Omega, \end{aligned} \tag{64}$$

and is extended as zero outside. Then, U_2 solves equation

$$\begin{aligned} \Delta U_2 &= 0, \quad \mathbf{x} \in \Omega, \\ [U_2] &= U_1, \quad \mathbf{x} \in \partial\Omega, \\ \left[\frac{\partial U_2}{\partial \nu}\right] &= 0, \quad \mathbf{x} \in \partial\Omega. \end{aligned} \tag{65}$$

The solution to (65) is given by the double layer potential

$$U_2(\mathbf{x}) = \int_{\partial\Omega} U_1(\mathbf{y}) \frac{\partial N}{\partial \nu}(\mathbf{x} - \mathbf{y})\, d\sigma(\mathbf{y}), \tag{66}$$

where N is the Newtonian potential in free space.

A different approach has been presented in [76], where U_1 is chosen to satisfy the equation

$$\begin{aligned} \Delta U_1 &= \text{div } \mathbf{M}, \quad \mathbf{x} \in \Omega, \\ U_1 &= 0, \quad x \in \partial\Omega, \end{aligned} \tag{67}$$

and it contains the bulk contribution of div $\mathbf{M}$ to the stray field. The function U_1 is extended to be equal to zero outside Ω.

The boundary contributions are included in U_2, which satisfies the equation

$$\begin{aligned} \Delta U_2 &= 0, \quad \mathbf{x} \in \Omega \cup \overline{\Omega}^c, \\ [U_2] &= 0, \ \mathbf{x} \in \partial\Omega, \\ \left[\frac{\partial U_2}{\partial \nu}\right] &= -\mathbf{m}\cdot\nu + \frac{\partial U_1}{\partial \nu}, \ \mathbf{x} \in \partial\Omega. \end{aligned} \tag{68}$$

The solution to (68) is

$$U_2(\mathbf{x}) = \int_{\partial\Omega} N(\mathbf{x}-\mathbf{y}) g(\mathbf{y})\, d\sigma(\mathbf{y}), \tag{69}$$

where $g(\mathbf{y}) = -\mathbf{M}\cdot\nu + \frac{\partial U_1}{\partial \nu}$.

The boundary values of U_2 can be evaluated using the integral representations (66) [74] or (69) [76], and therefore U_2 can be determined inside the domain solving a Poisson equation with Dirichlet boundary conditions.

In [76], the integral (69) is approximated on the boundary of the domain by approximating g using piece-wise polynomial interpolation. The corresponding moments of the Newtonian potential can be evaluated analytically. In two dimensions, the resulting sum can be evaluated in $O(N)$ operations by direct summation, where N is the total number of grid points in the domain, if a uniform grid was used. In three dimensions, however, the evaluation of the boundary values by direct summation is an $O(N^{\frac{4}{3}})$ operation. Solving Poisson's equation with Multigrid [77] is an $O(N)$ operation. Therefore, in two dimensions this procedure has optimal complexity. In three dimensions, the evaluation of the boundary values by direct summation dominates the CPU time. The computational time can be further reduced using a fast summation technique [78, 79, 80].

3.2. Fast Summation Techniques

For the fast summation of the stray field, the convolution integral in (10) is replaced by some numerical quadrature. The evaluation of (10) by direct summation requires $O(N^2)$ operations, where N is the number of grid points in the discretization. This becomes prohibitively expensive even for coarse discretizations. A number of fast summation techniques have appeared in the literature, such as the Tree-Code [81], or the Fast Multipole Method [78, 82], which reduce the computational cost to $O(N \log_2 N)$, or even $O(N)$. However,

for rectangular domains, the Fast Fourier Transform (FFT) [83] seems to be the most commonly used approach [84, 85]. It relies on the fact that when the integral (10) is approximated on a uniform grid with a quadrature rule, the resulting sum is a discrete convolution, with a kernel that is invariant under translation. The discrete convolution theorem applies [86], and the sum can be evaluated in $O(N \log_2 N)$ using the FFT.

For more general geometries, a common practice in micromagnetics has been to still use a regular grid, which results in a staircase approximation to the boundary. It was shown in [87] that this approach suffers from serious inaccuracies when the boundary $\partial\Omega$ cuts through numerical cells. The approach presented in [87] consists on decomposing the stray field into two contributions: a far field, and a near field. The near field is treated with direct summation, and it takes into account the geometry of the domain. For the far field, the contribution from the boundary cells is approximated to leading order by a rectangular cell with a properly scaled magnetization, in a way reminiscent of the Tree-Code, or the Fast Multipole Method. The resulting sum is evaluated using the FFT.

It is important to note that a significant speedup can be achieved in the study of thin ferromagnetic films. Due to the potential of thin films in applications, these films have been studied both experimentally, and analytically [88, 89, 90, 91, 20, 22, 92, 17, 71, 19, 93, 94]. For a thin domain of the form $\Omega = V \times [0, \delta]$, with $\delta \ll \text{diam}\,(V)$, the magnetization is independent of the thickness variable to leading order in δ [91]. Then, the stray field can be written as [17, 19]

$$E_s[\mathbf{m}] = \frac{\delta}{2} \int_V \mathbf{m}' \nabla \left(\nabla K_\delta * \mathbf{m}' \right) + \frac{\delta}{2} \int_V m_3 \left(W_\delta * m_3 \right), \tag{70}$$

where $\mathbf{m}' = (m_1, m_2)$ are the in-plane components of the magnetization, and m_3 is the out-of-plane component. The convolution kernels in (70) are defined as

$$K_\delta(\mathbf{x}) = -\left(\frac{1}{2\pi} \operatorname{senh}^{-1}\left(\frac{\delta}{|\mathbf{x}|} \right) - \frac{1}{2\pi\delta} \left(\sqrt{|\mathbf{x}|^2 + \delta^2} - |\mathbf{x}| \right) \right), \tag{71}$$

$$W_\delta(\mathbf{x}) = \frac{1}{2\pi\delta} \left(\frac{1}{|\mathbf{x}|} - \frac{1}{\sqrt{|\mathbf{x}|^2 + \delta^2}} \right). \tag{72}$$

The energy (70) can be written in Fourier space as

$$E_s[\mathbf{m}] = \frac{\delta}{2} \int_{\mathbb{R}^2} \frac{|\xi \cdot \widehat{\mathbf{m}'}|^2}{|\xi|^2} \left(1 - \widehat{\Gamma_\delta}(\xi) \right) d\xi + \frac{\delta}{2} \int_{\mathbb{R}^2} |\widehat{m_3}|^2 \widehat{\Gamma_\delta}(\xi)\, d\xi, \tag{73}$$

where

$$\widehat{\Gamma_\delta}(\eta) = \frac{1 - e^{-2\pi\delta|\eta|}}{2\pi\delta|\eta|}, \quad \eta \in \mathbb{R}^2. \tag{74}$$

This model was used in [17, 87, 71] for the study of thin ferromagnetic films.

A similar procedure can be carried out for a double layer consisting of two thin ferromagnetic layers of thicknesses D_1 and D_2, respectively, separated by a non-magnetic layer of thickness a. In this case the stray field energy becomes

$$\begin{aligned}
2E_s[\mathbf{m}_1,\mathbf{m}_2] &= D_1\int_\Omega \mathbf{m}_1'\nabla\left(\nabla K_1 * \mathbf{m}_1'\right) + D_1\int_\Omega m_{1,3}\left(W_1 * m_{1,3}\right)\\
&+ D_2\int_\Omega \mathbf{m}_2'\nabla\left(\nabla K_2 * \mathbf{m}_2'\right) + D_2\int_\Omega m_{2,3}\left(W_2 * m_{2,3}\right)\\
&+ D_1D_2\int_\Omega \mathbf{m}_1'\nabla\left(\nabla \Psi_{D_1,D_2,a} * \mathbf{m}_2'\right) - D_1D_2\int_\Omega m_{1,3}\Sigma_{D_1,D_2,a} * m_{2,3}\\
&+ D_1D_2\int_\Omega \left(m_{2,3}\nabla\Theta_{D_1,D_2,a} * \mathbf{m}_1' - m_{1,3}\nabla\Theta_{D_1,D_2,a} * \mathbf{m}_2'\right), \quad (75)
\end{aligned}$$

where

$$\begin{aligned}
K_j(\mathbf{x}) &= -\left(\frac{1}{2\pi}\,\mathrm{senh}^{-1}\left(\frac{D_j}{|\mathbf{x}|}\right) - \frac{1}{2\pi D_j}\left(\sqrt{|\mathbf{x}|^2+D_j^2}-|\mathbf{x}|\right)\right),\\
W_j(\mathbf{x}) &= \frac{1}{2\pi D_j}\left(\frac{1}{|\mathbf{x}|} - \frac{1}{\sqrt{|\mathbf{x}|^2+D_j^2}}\right),\\
\Psi_{D_1,D_2,a}(\mathbf{x}) &= -\frac{1}{2\pi D_1D_2}\Bigg(2a\,\mathrm{senh}^{-1}\left(\frac{2a}{|\mathbf{x}|}\right) + (2a+D_1+D_2)\,\mathrm{senh}^{-1}\left(\frac{2a+D_1+D_2}{|\mathbf{x}|}\right)\\
&\quad -(2a+D_1)\,\mathrm{senh}^{-1}\left(\frac{2a+D_1}{|\mathbf{x}|}\right)\\
&\quad -(2a+D_2)\,\mathrm{senh}^{-1}\left(\frac{2a+D_2}{|\mathbf{x}|}\right) + \sqrt{|\mathbf{x}|^2+(2a+D_1)^2}\\
&\quad +\sqrt{|\mathbf{x}|^2+(2a+D_2)^2} - \sqrt{|\mathbf{x}|^2+4a^2} - \sqrt{|\mathbf{x}|^2+(2a+D_1+D_2)^2}\Bigg),\\
\Sigma_{D_1,D_2,a}(\mathbf{x}) &= \frac{1}{2\pi D_1D_2}\left(\frac{1}{\sqrt{|\mathbf{x}|^2+4a^2}} - \frac{1}{\sqrt{|\mathbf{x}|^2+(2a+D_1)^2}}\right.\\
&\quad \left. -\frac{1}{\sqrt{|\mathbf{x}|^2+(2a+D_2)^2}} + \frac{1}{\sqrt{|\mathbf{x}|^2+(2a+D_1+D_2)^2}}\right),\\
\Theta_{D_1,D_2,a}(\mathbf{x}) &= \frac{1}{2\pi D_1D_2}\left(\mathrm{senh}^{-1}\left(\frac{2a+D_1}{|\mathbf{x}|}\right) + \mathrm{senh}^{-1}\left(\frac{2a+D_2}{|\mathbf{x}|}\right)\right.\\
&\quad \left. -\mathrm{senh}^{-1}\left(\frac{2a}{|\mathbf{x}|}\right) - \mathrm{senh}^{-1}\left(\frac{2a+D_1+D_2}{|\mathbf{x}|}\right)\right).
\end{aligned}$$

Alternatively, in Fourier space

$$
\begin{aligned}
2E_s[\mathbf{m}_1,\mathbf{m}_2] = D_1 \int_{\mathbb{R}^2} \frac{|\xi\cdot\widehat{\mathbf{m}_1'}|^2}{|\xi|^2}\left(1-\widehat{\Gamma_1}(\xi)\right)\,d\xi + D_1\int_{\mathbb{R}^2}|\widehat{m_{1,3}}|^2\widehat{\Gamma_1}(\xi)\,d\xi \\
+ D_2 \int_{\mathbb{R}^2} \frac{|\xi\cdot\widehat{\mathbf{m}_2'}|^2}{|\xi|^2}\left(1-\widehat{\Gamma_2}(\xi)\right)\,d\xi + D_2\int_{\mathbb{R}^2}|\widehat{m_{2,3}}|^2\widehat{\Gamma_2}(\xi)\,d\xi \\
+ 2\pi D_1 D_2 \Re\int_{\mathbb{R}^2}(\xi\cdot\widehat{\mathbf{m}_1'})\overline{(\xi\cdot\widehat{\mathbf{m}_2'})}\frac{e^{-4\pi a|\xi|}}{|\xi|}\widehat{\Gamma_1}(\xi)\widehat{\Gamma_2}(\xi)\,d\xi \\
- 2\pi D_1 D_2 \Im\int_{\mathbb{R}^2}\left((\xi\cdot\widehat{\mathbf{m}_1'})\overline{\widehat{m_{2,3}}} + \overline{(\xi\cdot\widehat{\mathbf{m}_2'})}\widehat{m_{1,3}}\right)e^{-4\pi a|\xi|}\widehat{\Gamma_1}(\xi)\widehat{\Gamma_2}(\xi)\,d\xi \\
- 2\pi D_1 D_2 \Re\int_{\mathbb{R}^2}\widehat{m_{1,3}}\overline{\widehat{m_{2,3}}}|\xi|e^{-4\pi a|\xi|}\widehat{\Gamma_1}(\xi)\widehat{\Gamma_2}(\xi)\,d\xi. \quad (76)
\end{aligned}
$$

The model (75) has been used by the author to characterize the Bloch and Néel walls in double layers [95, 96].

4. Energy Minimization Algorithms

When one is interested only in the local minimizers of the Landau-Lifshitz energy (13), an energy minimization algorithm can be used, instead of a dynamic approach. The first such approach in Micromagnetics is due to Brown and Labonte [97]. The method is based on the fixed point iteration

$$
\mathbf{m}_i^{n+1} = \frac{\mathbf{h}_i^n}{|\mathbf{h}_i^n|}, \quad (77)
$$

where the effective field $\mathbf{h}$ is given by (24). The algorithm suffers from a very slow convergence, specially when fine grids are used. Although the method can be accelerated using a Gauss-Seidel, or a SOR approach [98], the convergence is still too slow for practical purposes.

In order to carry out realistic computations, a more efficient method is needed. One of the simplest approaches is the Steepest Descent method, which in this contexts is equivalent to removing the gyromagnetic term in the Landau-Lifshitz equation. As is typical in these cases, linear convergence to a critical point is achieved.

For faster convergence, commonly used methods are the Nonlinear Conjugate Gradient (NCG), which achieves super-linear convergece, and Truncated Newton methods, which can achieve local quadratic convergence [99].

4.1. Nonlinear Conjugate Gradient

In Micromagnetics the NCG has been frequently used, mostly because it only requires the computation of the gradient of the energy, as opposed to the Newton method, where the Hessian of the energy is required. The unit length constraint $|\mathbf{m}| = 1$ is usually imposed by rewriting the energy in polar

coordinates [75]. One of the difficulties in this approach is that the resulting Laplacian term in the gradient does not have constant coefficients.

Define $\mathbf{m} = (\text{sen}(\theta)\cos(\phi), \text{sen}(\theta)\,\text{sen}(\psi), \cos(\theta))$. The Landau-Lifshitz energy (22) becomes

$$\begin{aligned} F_{LL}[\theta,\psi] &= \frac{q}{2}\int_\Omega (1-\text{sen}^2(\theta)\cos^2(\psi))\,d\mathbf{x} + \frac{\epsilon}{2}\int_\Omega (|\nabla\theta|^2 + |\nabla\psi|^2\,\text{sen}^2(\theta))\,d\mathbf{x} \\ &- \int_\Omega \left(\frac{1}{2}\mathbf{h}_s + \mathbf{h}_e\right)\cdot(\text{sen}(\theta)\cos(\phi), \text{sen}(\theta)\,\text{sen}(\psi), \cos(\theta))\,d\mathbf{x}. \quad (78) \end{aligned}$$

The energy is discretized using finite differences or finite elements, and the discrete energy is minimized.

The NCG method mimics the method of Conjugate Gradients (CG) for linear, symmetric, positive definite systems designed by Hestenes and Stiefel [100]. As in the CG, in the NCG a sequence of approximations $(\theta^{(k)}, \phi^{(k)})$ is constructed, as well as a sequence of descent directions, $(\mathbf{p}^{(k)}, \mathbf{q}^{(k)})$, satisfiying

$$\nabla F_{LL}[\theta^{(k)}, \phi^{(k)}]\cdot(\mathbf{p}^{(k)}, \mathbf{q}^{(k)}) < 0, \quad (79)$$

where $\nabla F_{LL} = (\nabla_\theta F_{LL}, \nabla_\psi F_{LL})$. Given an approximation to the minimizer and a descent direction, the function $F_{LL}[\theta^{(k)} + \alpha\mathbf{p}^{(k)}, \psi^{(k)} + \alpha\mathbf{q}^{(k)}]$ is approximately minimized. This procedure is known as *line search*, and it produces α_k. The next approximation is $(\theta^{(k+1)}, \phi^{(k+1)}) = (\theta^{(k)}, \phi^{(k)}) + +\alpha_k(\mathbf{p}^{(k)}, \mathbf{q}^{(k)})$. The next descent direction is defined, similarly to the CG case, as

$$(\mathbf{p}^{(k+1)}, \mathbf{q}^{(k+1)}) = -\nabla F_{LL}[\theta^{(k+1)}, \psi^{(k+1)}] + \beta_{k+1}(\mathbf{p}^{(k)}, \mathbf{q}^{(k)}). \quad (80)$$

There are several choices for the constant β_{k+1} in (80), and each one gives origin to a different variant of the NCG. The most commonly used are

$$\beta_{k+1}^{FR} = \frac{(\nabla F_{LL}[\mathbf{m}^{(k+1)}], \nabla F_{LL}[\mathbf{m}^{(k+1)}])}{(\nabla F_{LL}[\mathbf{m}^{(k)}], \nabla F_{LL}[\mathbf{m}^{(k)}])}, \quad (81)$$

which defines the Fletcher-Reeves method;

$$\beta_{k+1}^{PR} = \frac{(\nabla F_{LL}[\mathbf{m}^{(k+1)}], \nabla F_{LL}[\mathbf{m}^{(k+1)}] - \nabla F_{LL}[\mathbf{m}^{(k)}])}{(\nabla F_{LL}[\mathbf{m}^{(k)}], \nabla F_{LL}[\mathbf{m}^{(k)}])}, \quad (82)$$

which is known as the Polak-Ribiére method, and

$$\beta_{k+1}^{HS} = \frac{(\nabla F_{LL}[\mathbf{m}^{(k+1)}], \nabla F_{LL}[\mathbf{m}^{(k+1)}] - \nabla F_{LL}[\mathbf{m}^{(k)}])}{(\mathbf{p}^{(k)}, \nabla F_{LL}[\mathbf{m}^{(k)}] - \nabla F_{LL}[\mathbf{m}^{(k)}])}, \quad (83)$$

which defines the Hestenes-Stiefel method. For simplicity, in (81), (82), and (83), we have used the notation $\mathbf{m}^{(k+1)}$ and $\mathbf{m}^{(k)}$ to represent the magnetization obtained with $(\theta^{(k+1)}, \psi^{(k+1)})$ and $(\theta^{(k)}, \psi^{(k)})$, respectively.

In order to ensure that the new direction $(\mathbf{p}^{(k+1)}, \mathbf{q}^{(k+1)})$ is a direction of descent in the Fletcher-Reeves method, the strong Wolfe condition needs to be imposed on α:

$$\begin{aligned} F_{LL}[\mathbf{m}^{(k+1)}] &\leq F_{LL}[\mathbf{m}^{(k)}] + c_1\alpha_k \nabla F_{LL}[\mathbf{m}^{(k)}] \cdot (\mathbf{p}^{(k)}, \mathbf{q}^{(k)}), \\ |\nabla F_{LL}[\mathbf{m}^{(k+1)}] \cdot (\mathbf{p}^{(k)}, \mathbf{q}^{(k)})| &\leq c_2 |\nabla F_{LL}[\mathbf{m}^{(k)}] \cdot (\mathbf{p}^{(k)}, \mathbf{q}^{(k)})|, \end{aligned} \tag{84}$$

where $0 < c_1 < c_2 < \frac{1}{2}$. Additional conditions must be imposed to ensure that the new $(\mathbf{p}^{(k+1)}, \mathbf{q}^{(k+1)})$ is a direction of descent for the Polak-Ribiére and the Hestenes-Stiefel method [99].

4.2. Truncated Newton Method

Newton-based methods have been very successful in large-scale unconstrained minimization problems [101, 99]. We present here a modification of the Truncated-Newton method appropriate for constrained minimization, under the pointwise constraint $|\mathbf{m}(\mathbf{x})| = 1$.

In the Truncated-Newton described here, we again define a sequence of approximations $\{\mathbf{m}^{(k)}\}$, and a sequence of descent directions, $\{\mathbf{p}^{(k)}\}$. In order to obtain a new descent direction, the energy is approximated around $\mathbf{m}^{(k)}$ by a quadratic functional, which is subsequently minimized. The new approximation is $\mathbf{m}^{(k+1)} = \mathbf{m}^{(k)} + \alpha \mathbf{p}^{(k)}$, where α is usually chosen performing a line search.

This algorithm has been implemented in cartesian coordinates, without the need to rewrite the energy in polar coordinates [17, 19, 95, 96]. In order to impose the constraint $|\mathbf{m}(\mathbf{x})| = 1$, the energy is approximated, locally, by a quadratic functional:

$$F_{LL}\left[\frac{\mathbf{m}+\mathbf{p}}{|\mathbf{m}+\mathbf{p}|}\right] = F_{LL}[\mathbf{m}] + (G[\mathbf{m}], \mathbf{p})_h + \frac{1}{2}(H[\mathbf{m}] \cdot \mathbf{p}, \mathbf{p})_h + O(|\mathbf{p}|^3). \tag{85}$$

In minimization without constraints, G and H are the gradient and Hessian of the energy, respectively. In the constrained problem, G and H are projected versions of the gradient and Hessian, respectively. The projected gradient is

$$G[\mathbf{m}]_i = \Pi_{\mathbf{m}_i}(\mathcal{H}[\mathbf{m}]_i) = \mathcal{H}[\mathbf{m}]_i - (\mathcal{H}[\mathbf{m}]_i, \mathbf{m}_i)\,\mathbf{m}_i. \tag{86}$$

In (86) $\Pi_{\mathbf{m}}$ denotes the projection operator defined by $\Pi_m(v) = v - (u \cdot m)\mathbf{m}$. Therefore, $\mathbf{m} \cdot \Pi_m(v) = 0$.

In practice, often we do not need to compute the Hessian explicitly, but rather the action of the Hessian on a vector, which can be obtained from (85):

$$\begin{aligned} (H[\mathbf{m}] \cdot \mathbf{p})_i = \Pi_{\mathbf{m}_i} \sum_j \frac{\partial^2 F_{LL}}{\partial \mathbf{m}_i \partial \mathbf{m}_j}[\mathbf{m}] \cdot \Pi_{\mathbf{m}_j}(\mathbf{p}_j) - (G[\mathbf{m}]_i, \mathbf{p}_i)\mathbf{m}_i \\ - (\mathbf{m}_i, \mathbf{p}_i) G[\mathbf{m}]_i - \left(\frac{\partial F_{LL}}{\partial \mathbf{m}_i}[\mathbf{m}], \mathbf{m}_i\right) \Pi_{\mathbf{m}_i}(\mathbf{p}_i). \end{aligned} \tag{87}$$

The Euler-Lagrange equation is $G[\mathbf{m}] = 0$, or

$$\nabla F_{LL}[\mathbf{m}]_i = \left(\frac{\partial F_{LL}}{\partial \mathbf{m}_i}[\mathbf{m}], \mathbf{m}_i \right) \mathbf{m}_i. \tag{88}$$

When we minimize the quadratic part of (85), we obtain that $\mathbf{p}$ satisfies the linear equation

$$H[\mathbf{m}] \cdot \mathbf{p} = -G[\mathbf{m}]. \tag{89}$$

The matrix $H[\mathbf{m}]$ is symmetric, but not necessarily positive definite. We use the Preconditioned Conjugate Gradient (PCG) to solve equation (89). For the preconditioner we use the Laplacian term, which in our discretization can be inverted using the FFT. If $H[\mathbf{m}]$ is not positive definite, the procedure fails by producing a direction of negative curvature. In that case we use the corresponding approximation to the solution of system (89) as our descent direction. Sufficiently near the minimum, $H[\mathbf{m}]$ becomes positive definite, and from (89) we get $\mathbf{p} = -H[\mathbf{m}]^{-1} \cdot G[\mathbf{m}]$, i.e., Newton's method. For details regarding the convergence of this algorithm in the unconstrained case, see [99].

Given an approximation to the minimizer of (13), $\mathbf{m}^{(k)}$, and a descent direction, $\mathbf{p}$, the next approximation is computed with a line search using

$$f(\epsilon) = F_{LL} \left[\frac{\mathbf{m}^{(k)} + \epsilon \mathbf{p}}{|\mathbf{m}^{(k)} + \epsilon \mathbf{p}|} \right]. \tag{90}$$

In order to ensure sufficient decrease in the energy, the Wolf conditions need to be imposed [99].

5. Thermal Effects

Thermal effects have been shown to be important during the magnetization reversal process in sub-micron sized magnetic samples [102, 103], and have been the subject of much study recently [104, 105, 106, 107, 108, 109, 110, 93, 111]. Noise becomes more important in smaller samples, since the energy barrier heights decrease as the sample volume is reduced. Thermal noise depends only on the temperature, and therefore thermal effects may become dominant in samples with very small grain size. This affects negatively the reliability of magnetic storage devices, such as hard drives, and MRAMs, and represents one of the biggest challenges the magnetic recording industry is facing these days. From the technological point of view, the main difficulty in the design of effective MRAMs is the occurrence of rare events, which can spontaneously trigger the reversal of the magnetization, effectively erasing the information stored.

Traditionally, thermal effects have been studied using Monte Carlo methods, or by direct simulation of the Langevin equation (19). Due to the disparity of the deterministic time-scale, and the time-scale of the rare events, these methods result prohibitively expensive. A number of alternative methods have appeared in the literature in the past few years, the most notable being the Minimum Action Method [107, 109], and the String Method [105, 106, 109]. We will briefly

discuss some of these here, and refer to the original articles for a more detail analysis.

5.1. Time-Stepping methods for the stochastic Landau-Lifshitz equation

A common approach for the simulation of the stochastic LLE (19) is the natural extension of the methods described in section 2 for the deterministic equation. The white noise term is replaced by

$$\epsilon\dot{\mathcal{W}} \to \frac{\epsilon}{\sqrt{\Delta V}\sqrt{\Delta t}} N(0,1)_{ijk}, \tag{91}$$

where $\Delta V = \Delta x \Delta y \Delta z$ is the unit cell volume of the grid, Δt is the time step size, and $N(0,1)$ is a random variable with a normal distribution with mean zero, and variance one. A value of the random variable is generated at every cell, and at every time step, and the values in different cells are independent of each other. The time stepping proceeds as in the deterministic case.

The stability of the numerical methods suffer a more stringent constraint in the deterministic case. For example, the numerical integration of the stochastic Landau-Lifshitz equation using the Heun method, for a cell size $\Delta x = 0.006\,\mu m$, requires a time step size $\Delta t \approx 0.1$ femtoseconds [112]. To alleviate the stability constraints, implicit schemes are desirable. The GSPM has been tested for the stochastic equation, and it was shown to retain the properties described earlier in the deterministic case [71]. With this method it is possible to carry out fully resolved simulations of the stochastic Landau-Lifshitz equations (equation (19) below), with time step size $\Delta t = 1$ picosecond, for a cell size $\Delta x = 0.004\,\mu m$, an improvement of approximately four orders of magnitude in the time step size required, compared to explicit time stepping methods.

5.2. Study of Rare Events

A number of numerical procedures for the study of rare events are based on the theory of Wentzell and Freidlin [113] for large deviations. The starting point of this theory is a stochastic ordinary differential equation of the form

$$\begin{aligned} dX_t^\eta &= b(X_t^\eta)dt + \sqrt{\eta}d\mathcal{W}_t, \\ X_0^\eta &= x_0, \end{aligned} \tag{92}$$

where $0 < \eta \ll 1$, and $\mathcal{W}_t$ is a Wiener process in $\mathbb{R}^n$. As $\eta \to 0$, the trajectory X_t^η converges in probability to the solution of the deterministic equation, which we denote by $\varphi(t)$. We will assume that $b(X)$ is a Lipschitz continuous function, to ensure uniqueness of the solution to the deterministic ODE.

Define $C([0,T];\mathbb{R}^n)$, the set of continuous functions on the interval $[0,T]$ with values in $\mathbb{R}^n$, and in that space, the following metri:

$$d(\phi,\psi) = \sum_{0\le t\le T} \|\phi(t) - \psi(t)\|. \tag{93}$$

The theory of Wentzell and Freidlin gives an estimate on the probability that the stochastic process X_t^η stays inside a cylinder of radius δ around the deterministic solution:

$$P\left(d(X^\eta, \varphi) < \delta\right) \approx \exp\left\{\frac{1}{\eta} S_{0,T}(\varphi)\right\}, \tag{94}$$

where $S_{0,T}(\varphi)$ is called the *action functional*, and is defined by

$$S_{0,T}(\phi) = \frac{1}{2}\int_0^T |\dot{\varphi} - b(\phi)|^2 \, dt. \tag{95}$$

For the precise meaning of (94), we refer the reader to [113]. Note that (95) is only finite if φ is absolutely continuous.

Given two states $X(0) = a$ and $X(T) = b$, expression (94) can be used to determine the most likely path that the stochastic process will follow by minimizing the action:

$$S_{0,T}(\varphi^*) = \min_{\{\varphi \in C([0,T];\mathbb{R}^n),\ \varphi(0)=a,\ \varphi(T)=b\}} S_{0,T}(\varphi). \tag{96}$$

Such a path is called *minimal action path* (MAP). When the system is a gradient system, then the minimal action path becomes a minimal energy path (MEP).

Efficient methods have been developed for computing the MAP and the MEP, as well as the transition rates between different configurations [105, 106, 107, 109, 93, 114].

6. Acknowledgments

I would like to thank Weinan E, for introducing me to this area of research during my doctoral dissertation. Throughout the years I have greatly benefited from many discussions with Anthony Arrott, Antonio DeSimone, Leslie Greengard, Roger Koch, Robert V. Kohn, Di Liu, Felix Otto, Stefan Müller, Weiqing Ren, Xiao-Ping Wang, among many others that I ommit because of lack of space. This review represents a large portion of my work on micromagnetics. Part of my work described here was done under funding from NSF, grant numbers DMS-0505738 and DMS-0411504, and a Faculty Career Development Award from UCSB.

A. Ito vs Stratonovich interpretation of the Landau-Lifshitz-Langevin equation

When the Landau-Lifshitz-Langevin equation (19) is interpreted in the Ito sense, the length of the magnetization is not only not preserved, but it blows up in finite time. To see this, let us consider equation (19), rewritten in the following form:

$$d\mathbf{m}_t = \mathbf{f}(\mathbf{m})dt + \mathbf{G}(\mathbf{m}) \cdot d\mathbf{B}_t, \tag{97}$$

where $\mathbf{f}(\mathbf{m}) = -\mathbf{m}\times\mathbf{h} - \alpha\mathbf{m}\times(\mathbf{m}\times\mathbf{h})$, the matrix $\mathbf{G}(\mathbf{m})$ is defined as

$$\mathbf{G}(\mathbf{m}) = \epsilon \begin{pmatrix} 0 & m_3 & -m_2 \\ -m_3 & 0 & m_1 \\ m_2 & -m_1 & 0 \end{pmatrix} + \epsilon\alpha\left(|\mathbf{m}|^2\mathbf{I} - \mathbf{m}\otimes\mathbf{m}\right), \tag{98}$$

and $\mathbf{B}_t$ denotes a three-dimensional Wiener process. According to Ito's formula [55],

$$\begin{aligned} d|\mathbf{m}|^2 &= 2\mathbf{m}\cdot d\mathbf{m} + \sum_{i,j}\delta_{i,j}dm_i dm_j = \sum_i (dm_i)^2 = \sum_{i,k}(G_{ik})^2 dt \\ &= 2\epsilon^2(|\mathbf{m}|^2 + \alpha^2|\mathbf{m}|^4)dt. \end{aligned} \tag{99}$$

Therefore, $y(t) = |\mathbf{m}|^2(t)$ solves the deterministic equation, with random initial data:

$$\begin{aligned} \frac{dy}{dt} &= 2\epsilon^2(y + \alpha^2 y^2) \\ y(0) &= |\mathbf{m}_0|^2. \end{aligned} \tag{100}$$

The solution is

$$|\mathbf{m}|^2(t) = \frac{Ce^{2\epsilon^2 t}}{1 - \alpha C e^{2\epsilon^2 t}}, \tag{101}$$

where C is defined in such a way that $y(0) = |\mathbf{m}_0|^2$:

$$C = \frac{|\mathbf{m}_0|^2}{1 + \alpha|\mathbf{m}_0|^2}. \tag{102}$$

Therefore the length of the magnetization becomes infinite at time

$$t^* = \frac{1}{2\epsilon^2}\log\frac{1}{\alpha C} > 0. \tag{103}$$

Consequently, equation (19) must be understood in the sense of Stratonovich.

References

[1] L. Landau and E. Lifshitz. On the theory of the dispersion of magnetic permeability in ferromagnetic bodies. *Physikalische Zeitschrift der Sowjetunion*, 8:153–169, 1935.

[2] W.F. Brown Jr. *Micromagnetics*. Interscience Tracts on Physics and Astronomy. Interscience Publishers (John Wiley and Sons), New York - London, 1963.

[3] P. Weiss. L'hypothèse du champ moléculaire et la propriété ferromagnétique. *J. de Phys. Rad.*, 6:661–690, 1907. (*The hypothesis of the molecular field and the property of ferromagnetism*).

[4] W. Heisenberg. Zur Theorie des Ferromagnetismus. *Z. Phys*, 49:619–636, 1928. (*On the theory of ferromagnetism*).

[5] G.A. Prinz. Magnetoelectronics. *Science*, 282:1660–1663, 1998.

[6] M. Ziese and Martin J. Thornton (Eds.). *Spin Electronics*, volume 569 of *Lecture Notes in Physics*. Springer-Verlag, Berlin, Heidelberg, 2001.

[7] E. Hirota, H. Sakakima, and K. Inomata. *Giant Magneto-Resistance Devices*. Springer-Verlag, Berlin, Heidelberg, New York, 2002.

[8] I.B. Puchalska and H. Niedoba. Magnetization Process in Permalloy Multilayer Films. *IEEE Trans. Magn.*, 27:3579–3587, 1991.

[9] John David Jackson. *Classical electrodynamics*. John Wiley & Sons Inc., New York, second edition, 1975.

[10] Kōsaku Yosida. *Functional analysis*. Classics in Mathematics. Springer-Verlag, Berlin, 1995. Reprint of the sixth (1980) edition.

[11] W.F. Brown Jr. *Magnetoelastic interactions*, volume 9 of *Springer Tracts in Natural Philosophy*. Springer-Verlag, New York, 1966.

[12] R. D. James and D. Kinderlehrer. Frustration and microstructure: an example in magnetostriction. In *Progress in partial differential equations: calculus of variations, applications (Pont-à-Mousson, 1991)*, volume 267 of *Pitman Res. Notes Math. Ser.*, pages 59–81. Longman Sci. Tech., Harlow, 1992.

[13] Antonio DeSimone and Georg Dolzmann. Existence of minimizers for a variational problem in two-dimensional nonlinear magnetoelasticity. *Arch. Rational Mech. Anal.*, 144(2):107–120, 1998.

[14] Antonio DeSimone and Richard D. James. A constrained theory of magnetoelasticity. *J. Mech. Phys. Solids*, 50(2):283–320, 2002.

[15] I.A. Privorotskii. Thermodynamic theory of domain structures. *Rep. Prog. Phys.*, 35:115–155, 1972.

[16] Alex Hubert and Rudolf Schäfer. *Magnetic Domains: The Analysis of Magnetic Microstructures*. Springer-Verlag, Berlin-Heidelberg-New York, 1998.

[17] Carlos J. García-Cervera. *Magnetic Domains and Magnetic Domain Walls*. PhD thesis, Courant Institute of Mathematical Sciences, New York University, 1999.

[18] Rustum Choksi, Robert V. Kohn, and Felix Otto. Domain branching in uniaxial ferromagnets: a scaling law for the minimum energy. *Comm. Math. Phys.*, 201:61–79, 1999.

[19] C.J. García-Cervera. One-dimensional magnetic domain walls. *Euro. Jnl. Appl. Math.*, 15:451–486, 2004.

[20] Antonio DeSimone, Robert V. Kohn, Stefan Müller, and Felix Otto. Magnetic microstructures—a paradigm of multiscale problems. In *ICIAM 99 (Edinburgh)*, pages 175–190. Oxford Univ. Press, Oxford, 2000.

[21] F. Otto. Cross-over in scaling laws: a simple example from micromagnetics. In *Proceedings of the International Congress of Mathematicians*, volume 3, pages 829–838, Beijing, 2002. Higher Ed. Press.

[22] A. De Simone, R. V. Kohn, S. Müller, and F. Otto. Repulsive interaction of Néel walls, and the internal length scale of the cross-tie wall. *Multiscale Modeling and Simulation*, 1:57–104, 2003.

[23] A. DeSimone, H. Knöpfer, and F. Otto. 2-d stability of the Néel wall. *Calc. Var. and PDEs*, 27:233, 2006.

[24] T.L. Gilbert. *Phys. Rev.*, 100:1243, 1955. [Abstract only; full report, Armor Research Foundation Project No. A059, Supplementary Report, May 1, 1956 (unpublished)].

[25] P. Sulem, C. Sulem, and C. Bardos. On the continuous limit for a system of classical spins. *Comm. Math. Phys.*, 107(3):431–454, 1986.

[26] M. Lakshmanan and K. Nakamura. Landau-Lifshitz equation of ferromagnetism: Exact treatment of the gilbert damping. *Physical Review Letters*, 53(26):2497–2499, 1984.

[27] C. Kenig, G. Ponce, and L. Vega. Small solutions to nonlinear Schrödinger equations. *Ann. Inst. H. Poincaré Anal. Non Linéaire*, 10:255–288, 1993.

[28] C. Kenig, G. Ponce, and L. Vega. Smoothing effects and local existence theory forthe generalized nonlinear Schrödinger equations. *Invent. Math.*, 134:489–545, 1998.

[29] N. Hayashi and T. Ozawa. Remarks on nonlinear Schrödinger equations in one space dimension. *Diff. Integral Eqs.*, 2:453–461, 1994.

[30] H. Chihara. Local existence for semilinear Schrödinger equations. *Math. Japonica*, 42:35–52, 1995.

[31] N. Chang, J. Shatah, and K. Uhlenbeck. Schrödinger maps. *Comm. Pure Appl. Math.*, 53:590–602, 2000.

[32] Helena McGahagan. *Some Existence and Uniqueness Results for Schrödinger Maps and Landau-Lifshitz-Maxwell Equations*. PhD thesis, Courant Institute of Mathematical Sciences, New York University, 2004.

[33] Susana Gutiérrez, Judith Rivas, and Luis Vega. Formation of singularities and self-similar vortex motion under the localized induction approximation. *Comm. Partial Differential Equations*, 28(5-6):927–968, 2003.

[34] Susana Gutierrez and Luis Vega. Self-similar solutions of the localized induction approximation: singularity formation. *Nonlinearity*, 17(6):2091–2136, 2004.

[35] Michael Struwe. On the evolution of harmonic maps in higher dimensions. *Journal of Differential Geometry*, 28:485–502, 1988.

[36] Kung-Ching Chang, Wei Yue Ding, and Rugang Ye. Finite-time blow-up of the heat flow of harmonic maps from surfaces. *J. Differential Geom.*, 36(2):507–515, 1992.

[37] Roger Moser. *Partial regularity for harmonic maps and related problems*. World Scientific Publishing Co. Pte. Ltd., Hackensack, NJ, 2005.

[38] A. Visintin. On Landau-Lifshitz equations for ferromagnetism. *Japan J. Appl. Math.*, 2:69, 1985.

[39] F. Alouges and A. Soyeur. On global weak solutions for Landau-Lifshitz equations: Existence and nonuniqueness. *Nonlinear Analysis, Theory, Methods & Applications*, 18:1071–1084, 1992.

[40] G. Boling and S. Fengqiu. Global weak solution for the Landau-Lifshitz-Maxwell equation in three space dimensions. *J. Math. Anal. Appl.*, 211:326, 1987.

[41] J. Zhai. Existence and behaviour of solutions to the Landau-Lifshitz equation. *SIAM J. Math. Anal.*, 30:833, 1999.

[42] Xiaoming Wu. *Two dimensional Landau-Lifshitz equations in micromagnetism*. PhD thesis, Courant Institute of Mathematical Sciences, New York University, 2000.

[43] S. Gustafson and J. Shatah. The stability of localized solutions of Landau-Lifshitz equations. *Comm. Pure Appl. Math.*, 55:1136–1159, 2002.

[44] G. Carbou, P. Fabrie, and O. Gués. On the ferromagnetism equation in the non static case. *Comm. Pure Appl. Anal.*, to appear.

[45] G. Carbou and P. Fabrie. Recent results in micromagnetism. In *Colloque d'Analyse Numérique, Arles*, 1998.

[46] G. Carbou and P. Fabrie. Regular solutions for Landau-Lifschitz equation in a bounded domain. *Differential Integral Equations*, 14:213–229, 2001.

[47] G. Carbou and P. Fabrie. Regular solutions for Landau-Lifschitz equations in $\mathbb{R}^3$. *Comm. Appl. Anal.*, 5:17–30, 2001.

[48] Y. Chen. Existence and singularities for the Dirichlet boundary value problems of Landau-Lifshitz equations. *Nonlinear Analysis*, 48:411, 2002.

[49] Christof Melcher. Existence of partially regular solutions for Landau-Lifshitz equations in $\mathbb{R}^3$. *Comm. Partial Differential Equations*, 30(4):567–587, 2005.

[50] C.J. García-Cervera and X.P. Wang. Spin-Polarized transport: Existence of weak solutions. *Disc. Cont. Dyn. Sys., Series B*, 7(1):87–100, 2005.

[51] W.F. Brown Jr. Thermal Fluctuations of a Single-Domain Particle. *Physical Review*, 130(5):1677–1686, 1963.

[52] L. Garcia-Palacios and F.J. Lazaro. Langevin-dynamics study of the dynamical properties of small magnetic particles. *Phys. Rev. B*, 58:14937, 1998.

[53] G. Da Prato and J. Zabczyk. *Stochastic Equations in Infinite Dimensions*. Encyclopedia of Mathematics and Its Applications. Cambridge University Press, 1992.

[54] R. Kubo. The fluctuation-dissipation theorem. *Rep. Prog. Phys.*, 29:255–284, 1966.

[55] Bernt Øksendal. *Stochastic differential equations: An introduction with applications*. Universitext. Springer-Verlag, Berlin, sixth edition, 2003.

[56] J. Daughton. Magnetoresistive memory technology. *Thin Solid Films*, 216:162–168, 1992.

[57] J. Shi, T. Zhu, S. Tehrani, Y.F. Zheng, and J.-G. Zhu. Magnetization vortices and anomalous switching in patterned NiFeCo submicron arrays. *Applied Physics Letters*, 74:2525–2527, 1999.

[58] J. Shi and S. Tehrani. Edge pinned states in patterned submicron NiFeCo structures. *Applied Physics Letters*, 77(11):1692–1694, 2000.

[59] Y. Nakatani, Y. Uesake, and N. Hayashi. Direct solution of the Landau-Lifshitz-Gilbert equation for micromagnetics. *Japanese Journal of Applied Physics*, 28(12):2485–2507, 1989.

[60] C.J. García-Cervera. *Unpublished*.

[61] J. D. Lambert. *Computational methods in ordinary differential equations*. John Wiley & Sons, London-New York-Sydney, 1973. Introductory Mathematics for Scientists and Engineers.

[62] J.S. Jiang, H.G. Kaper, and G.K. Leaf. Hysteresis in layered spring magnets. *Discrete and Continuous Dynamical Systems - Series B*, 1:219–232, 2001.

[63] A. Iserles, editor. *Acta numerica. 2000*, volume 9 of *Acta Numerica*. Cambridge University Press, Cambridge, 2000.

[64] Feng Kang. On difference schemes and symplectic geometry. In Feng Kang, editor, *Proceedings of the 1984 Beijing Symposium on Differential Geometry and Differential Equations*, pages 42–58, Beijing, 1985. Science Press.

[65] J.J. Sanz-Serna. Symplectic integrators for hamiltonian problems: an overview. *Acta Numerica*, 1:243–286, 1991.

[66] D. Lewis and N. Nigam. Geometric integration on spheres and some interesting applications. *J. Comput. Appl. Math.*, 151(1):141–170, 2003.

[67] P.S. Krishnaprasad and X. Tan. Cayley transforms in micromagnetics. *Physica B*, 306:195–199, 2001.

[68] Jerrold E. Marsden and Tudor S. Ratiu. *Introduction to mechanics and symmetry*, volume 17 of *Texts in Applied Mathematics*. Springer-Verlag, New York, second edition, 1999. A basic exposition of classical mechanical systems.

[69] C. García-Cervera X.-P. Wang and W. E. A Gauss-Seidel projection method for micromagnetics simulations. *J. Comp. Phys.*, 171:357–372, 2001.

[70] Weinan E and X.P. Wang. Numerical methods for the Landau-Lifshitz equation. *SIAM J. Numer. Anal.*, 38(5):1647–1665, 2000.

[71] C. García-Cervera and W. E. Improved Gauss-Seidel projection method for micromagnetics simulations. *IEEE Transactions on Magnetics*, 39(3):1766–1770, May 2003.

[72] Semyon V. Tsynkov. Numerical solution of problems on unbounded domains. A review. *Appl. Num. Math.*, 27:465–532, 1998.

[73] W. Bao and H. Han. High-order local artificial boundary conditions for problems in unbounded domains. *Comput. Methods Appl. Mech. Engr.*, 188:455–471, 2000.

[74] T.R. Koehler and D.R. Fredkin. Finite element methods for micromagnetics. *IEEE Transactions on Magnetics*, 28:1239–1244, 1992.

[75] D.V. Berkov, K. Ramstöck, and A. Hubert. Solving micromagnetic problems: Towards an optimal numerical method. *Phys. Stat. Sol. (a)*, 137:207–225, 1993.

[76] C.J. García-Cervera and A.M. Roma. Adaptive mesh refinement for micromagnetics simulations. *IEEE Trans. Magn. Mag.*, 42:1648–1654, 2006.

[77] Briggs, W.L. *A Multigrid Tutorial*. SIAM – Society for Industrial and Applied Mathematics, 1987. Third Edition.

[78] L. Greengard and V. Rokhlin. A fast algorithm for particle simulations. *Journal of Computational Physics*, 73:325–348, 1987.

[79] J.L. Blue and M.R. Scheinfein. Using multipoles decreases computation time for magnetic self-energy. *IEEE Trans. Magn.*, 27:4778–4780, 1991.

[80] Nikola Popović and Dirk Praetorius. $\mathcal{H}$-matrix techniques for stray-field computations in computational micromagnetics. In *Large-scale scientific computing*, volume 3743 of *Lecture Notes in Comput. Sci.*, pages 102–110. Springer, Berlin, 2006.

[81] J. Barnes and P. Hut. A hierarchical $O(N \log(N))$ force calculation algorithm. *Nature*, 324:446–449, 1986.

[82] J. Carrier, L. Greengard, and V. Rokhlin. A fast adaptive multipole algorithm for particle simulations. *SIAM J. Sci. Stat. Comput.*, 9(4):669–686, 1988.

[83] James W. Cooley and John W. Tukey. An algorithm for the machine calculation of complex Fourier series. *Math. Comp.*, 19:297–301, 1965.

[84] Samuel W. Yuan and Neal Bertram. Fast adaptive algorithms for micromagnetics. *IEEE Transactions on Magnetics*, 28(5):2031–2036, 1992.

[85] N. Hayashi, K. Saito, and Y. Nakatani. Calculation of demagnetizing field distribution based on fast fourier transform of convolution. *Jpn. J. Appl. Phys.*, 35:6065–6073, 1996.

[86] Henri J. Nussbaumer. *Fast Fourier transform and convolution algorithms*, volume 2 of *Springer Series in Information Sciences*. Springer-Verlag, Berlin, 1981.

[87] C.J. García-Cervera, Z. Gimbutas, and W. E. Accurate numerical methods for micromagnetics simulations with general geometries. *J. Comp. Phys.*, 184(1):37–52, 2003.

[88] B. Heinrich and J.A.C. Bland. *Ultrathin Magnetic Structures I*. Springer-Verlag, Berlin-New York, 1994.

[89] B. Heinrich and J.A.C. Bland. *Ultrathin Magnetic Structures II*. Springer-Verlag, Berlin-New York, 1994.

[90] G. Bertotti and A. Magni. Landau-Lifshitz magnetization dynamics and eddy currents in metallic thin films. *J. Appl. Phys*, 91(10):7559–7561, 2002.

[91] Gustavo Gioia and Richard D. James. Micromagnetics of very thin films. *Proc. R. Soc. Lon. A*, 453:213–223, 1997.

[92] C. Melcher. The logarithmic tail of néel walls. *Arch. Rational Mech. Anal.*, 168, 2003.

[93] D. Liu and C.J. García-Cervera. Magnetic switching of thin films under thermal perturbation. *J. Appl. Phys.*, 98(023903), 2005.

[94] Robert V. Kohn and V.V. Slastikov. Effective dynamics for ferromagnetic thin films: rigurous justification. *Proc. Roy. Soc. London Ser. A*, to appear, 2004.

[95] C.J. García-Cervera. Néel Walls in Low Anisotropy Double Layers. *SIAM J. Appl. Math.*, 65(5):1726–1747, 2005.

[96] C.J. García-Cervera. Structure of the Bloch Wall in Multilayers. *Proc. R. Soc. A*, 461:1911–1926, 2005.

[97] W.F. Brown Jr. and A.E. LaBonte. Structure and energy of one dimensional walls in ferromagnetic thin films. *J. Appl. Phys.*, 36(4):1380–1386, 1965.

[98] K. Kosavisutte and N. Hayashi. A numericla study of LaBonte's iteration: An approach to acceleration. *IEEE Trans. Magn.*, 32:4243–4245, 1996.

[99] J. Nocedal and S.J. Wright. *Numerical Optimization*. Springer Series in Operations Research. Springer-Verlag, New York, 1999.

[100] Magnus R. Hestenes and Eduard Stiefel. Methods of conjugate gradients for solving linear systems. *J. Research Nat. Bur. Standards*, 49:409–436 (1953), 1952.

[101] R.S. Dembo and T. Steihaug. Truncated-newton algorithms for large-scale unconstrained optimization. *Mathematical Programming*, 26:190–212, 1983.

[102] R. H. Koch, G. Grinstein, G.A. Keefe, Yu Lu, P.L. Trouilloud, and W.J. Gallagher. Thermally Assisted Magnetization Reversal in Submicron-Sized Magnetic Thin Films. *Phys. Rev. Lett.*, 84(23):5419–5422, 2000.

[103] M. Bhattacharyya, T. Anthony, J. Nickel, M. Sharma, L. Tran, and R. Walmsley. Thermal Variations in Switching Fields for Sub-Micron MRAM Cells. *IEEE Trans. Mag.*, 37(4):1970–1972, 2001.

[104] X. Wang, H.N. Bertram, and V.L. Safonov. Thermal-dynamic reversal of fine magnetic grains with arbitrary anisotropy axes orientation. *J. Appl. Phys.*, 92(4):2064–2072, 2002.

[105] Weiqing Ren. *Numerical methods for the study of energy landscapes and rare events*. PhD thesis, Courant Institute of Mathematical Sciences, New York University, 2002.

[106] W. E, W. Ren, and E. Vanden-Eijnden. String method for the study of rare events. *Phys. Rev. B*, 66(5):2301, 2002.

[107] W. E, W. Ren, and E. Vanden-Eijnden. Energy landscape and thermally activated switching of submicron-sized ferromagnetic elements. *J. Appl. Phys.*, 93(4):2275, 2003.

[108] W. Ren. Higher order string method for finding minimun energy paths. *Comm. Math. Sci.*, 1(2):2377–384, 2003.

[109] W. E, W. Ren, and E. Vanden-Eijnden. Minimum action method for the study of rare events. *Comm. Pure Appl. Math.*, to appear, 2004.

[110] Di Liu. *Topics in the analysis and computation of stochastic differential equations*. PhD thesis, Program in Applied and Computational Mathematics, Princeton University, 2003.

[111] Maria G. Reznikoff. *Rare events in finite and infinite dimensions*. PhD thesis, Courant Institute of Mathematical Sciences, New York University, 2004.

[112] T. Schrefl, W. Scholz, D. Süs, and J. Fidler. Langevin micromagnetics of recording media using subgrain discretization. *IEEE Trans. Mag.*, 36:3189–3191, 2000.

[113] M. I. Freidlin and A. D. Wentzell. *Random perturbations of dynamical systems*, volume 260 of *Grundlehren der Mathematischen Wissenschaften [Fundamental Principles of Mathematical Sciences]*. Springer-Verlag, New York, second edition, 1998. Translated from the 1979 Russian original by Joseph Szücs.

[114] R.V. Kohn, M.G. Reznikoff, and E. Vanden-Eijnden. Magnetic elements at finite temperature and large deviation theory. *J. Nonlinear Sci.*, 15:225–253, 2005.

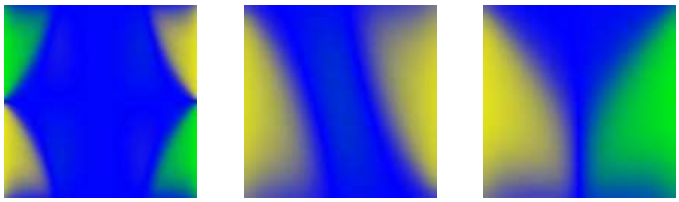

(a) Uniform state.

(b) S state.

(c) C State

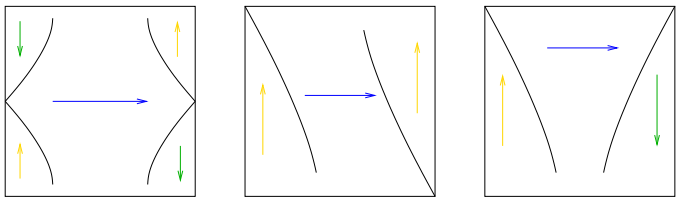

(d) Sketch of Uniform state.

(e) Sketch of S state.

(f) Sketch of C state.

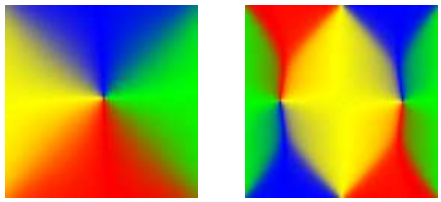

(g) Vortex state.

(h) Five Domains.

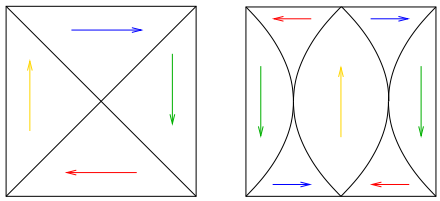

(i) Sketch of Vortex state.

(j) Sketch of Five Domains.

Figure 1: Different steady states of the magnetizatios. All the configurations have been obtained both by dynamic simulation of the Landau-Lifshitz equation, and by minimization of the Landau-Lifshitz energy using the Truncated Newton Method described in section 4. Under each configuration, we present a sketch depicting the average orientation of the magnetization in each domain.

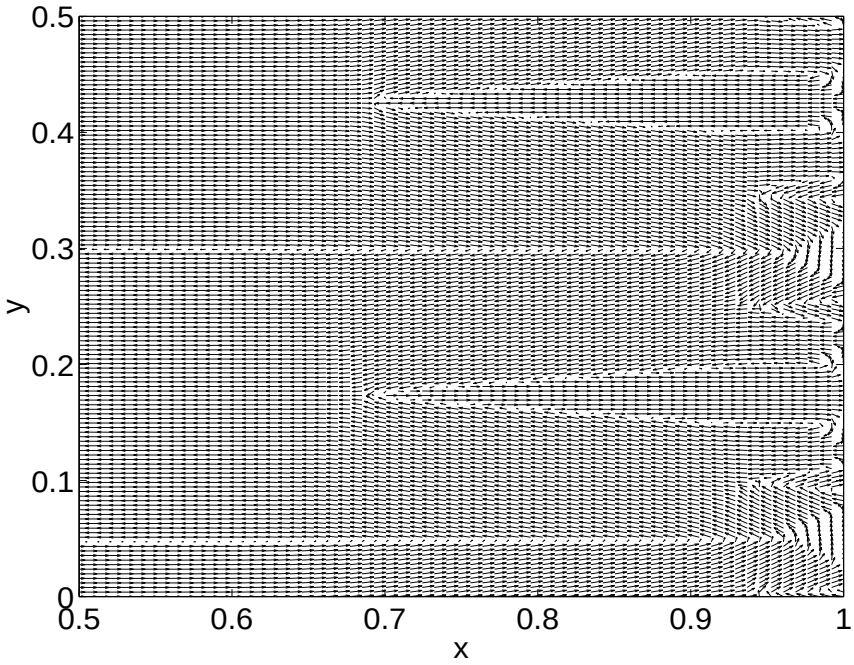

Figure 2: Branching structure near the boundary of a ferromagnet [18, 17].